



## First nanoparticles of $\text{Per}_2[\text{Au}(\text{mnt})_2]$

Dominique de Caro, Kane Jacob, Christophe Faulmann, Marine Tassé, Lydie Valade

### ► To cite this version:

Dominique de Caro, Kane Jacob, Christophe Faulmann, Marine Tassé, Lydie Valade. First nanoparticles of  $\text{Per}_2[\text{Au}(\text{mnt})_2]$ . *Comptes Rendus. Chimie*, 2020, 23 (4-5), pp.291-297. 10.5802/crchim.24 . hal-02978206

**HAL Id: hal-02978206**

**<https://hal.science/hal-02978206>**

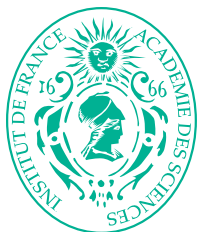
Submitted on 12 Nov 2020

**HAL** is a multi-disciplinary open access archive for the deposit and dissemination of scientific research documents, whether they are published or not. The documents may come from teaching and research institutions in France or abroad, or from public or private research centers.

L'archive ouverte pluridisciplinaire **HAL**, est destinée au dépôt et à la diffusion de documents scientifiques de niveau recherche, publiés ou non, émanant des établissements d'enseignement et de recherche français ou étrangers, des laboratoires publics ou privés.



Distributed under a Creative Commons Attribution 4.0 International License



INSTITUT DE FRANCE  
Académie des sciences

# *Comptes Rendus*

---

## *Chimie*


Dominique de Caro, Kane Jacob, Christophe Faulmann, Marine Tassé and Lydie Valade

**First nanoparticles of  $\text{Per}_2[\text{Au}(\text{mnt})_2]$**

Volume 23, issue 4-5 (2020), p. 291-297.

<<https://doi.org/10.5802/crchim.24>>

© Académie des sciences, Paris and the authors, 2020.  
*Some rights reserved.*

 This article is licensed under the  
CREATIVE COMMONS ATTRIBUTION 4.0 INTERNATIONAL LICENSE.  
<http://creativecommons.org/licenses/by/4.0/>



*Les Comptes Rendus. Chimie sont membres du  
Centre Mersenne pour l'édition scientifique ouverte*  
[www.centre-mersenne.org](http://www.centre-mersenne.org)



Preliminary communication / *Communication*

# First nanoparticles of $\text{Per}_2[\text{Au}(\text{mnt})_2]$

Dominique de Caro<sup>\*,a</sup>, Kane Jacob<sup>a</sup>, Christophe Faulmann<sup>a</sup>, Marine Tassé<sup>a</sup>  
and Lydie Valade<sup>a</sup>

<sup>a</sup> LCC-CNRS, Université de Toulouse, CNRS, UPS, Toulouse, France

E-mails: dominique.decaro@lcc-toulouse.fr (D. de Caro), kane.jacob@lcc-toulouse.fr (K. Jacob), christophe.faulmann@lcc-toulouse.fr (C. Faulmann), marine.tasse@lcc-toulouse.fr (M. Tassé), lydie.valade@lcc-toulouse.fr (L. Valade)

**Abstract.** Nanoparticles of the  $\text{Per}_2[\text{Au}(\text{mnt})_2]$  (Per = perylene;  $\text{mnt}^{2-}$  = maleonitrile dithiolate) compound have been obtained by the electrochemical oxidation of perylene in the presence of  $[(n\text{-C}_4\text{H}_9)_4\text{N}][\text{Au}(\text{mnt})_2]$  and, either an amphiphilic molecule (OATM), or a zwitterionic ionic liquid (BIBS), acting as growth controlling agents. When the reaction is carried out with OATM, nanocrystals exhibiting sizes in the 35–100 nm range are grown whereas roughly spherical nanoparticles are observed if BIBS is used (10–40 nm in diameter). Infrared and Raman spectra confirm the presence of both perylene donor and maleonitrile dithiolate ligands within the nanopowders. Electrical conductivity measurements at room temperature lead to about  $0.025 \text{ S}\cdot\text{cm}^{-1}$ , a typical value for nanopowders of bis(dithiolene)-based conducting compounds. Finally, current–voltage characteristics for the spherical nanoparticles are fitted with a Shockley diode model. A saturation current of 19.3 pA and a threshold voltage of 0.149 V are extracted from this model.

**Keywords.** perylene, maleonitrile dithiolate gold(III) complex, electrocrystallization, amphiphilic species, zwitterionic ionic liquid, nanoparticles, current–voltage curves.

*Manuscript received 25th February 2020, revised and accepted 23rd March 2020.*

## 1. Introduction

In 2010, our group described the first nanoparticles of a molecule-based conductor containing a bis(dithiolene) complex, *i.e.*,  $\text{TTF}[\text{Ni}(\text{dmit})_2]_2$  (TTF: tetrathiafulvalene,  $\text{dmit}^{2-}$ : 2-thioxo-1,3-dithiol-4,5-dithiolato) [1]. Nanoparticles were precipitated from an acetone/acetonitrile solution containing an imidazolium-based ionic liquid, acting as growth controlling agent. Thereafter,  $\text{TTF}[\text{Ni}(\text{dmit})_2]_2$  nanoparticles exhibiting a mean diameter of 20 nm were obtained by electrodeposition on a platinum wire in the presence of an ionic liquid, acting as

both supporting electrolyte and growth controlling agent [2]. In the series of bis(dithiolene) complexes,  $\text{M}(\text{mnt})_2$  (M = Fe, Co, Ni, Pd, Pt, Cu, Au;  $\text{mnt}^{2-}$ : maleonitrile dithiolate, Figure 1) have led to a wide variety of molecular conductors. Among them,  $\text{Per}_2[\text{Au}(\text{mnt})_2]$  (Per: perylene, Figure 1) is a low-dimensional molecular conductor which continues to attract great interest due to unusual physical properties, such as anisotropic field suppression of the charge density wave [3], or superconducting ground state under pressure [4].  $\text{Per}_2[\text{Au}(\text{mnt})_2]$  is usually obtained by the electrocrystallization technique leading to single crystals as thin needles (several millimeters long and small cross sections, typically  $0.05 \times 0.02 \text{ mm}^2$ ). This compound has also

\* Corresponding author.

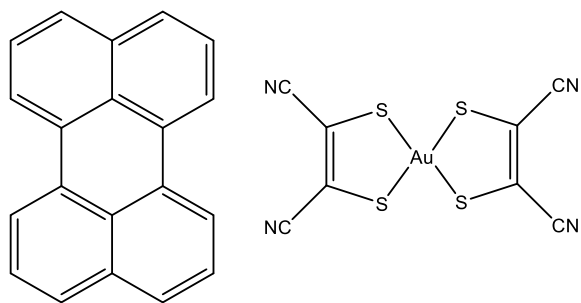


**Figure 1.** Formulas for perylene (left) and  $\text{Au}(\text{mnt})_2$  (right).

been grown as nano-sized needles on highly oriented pyrolytic graphite (HOPG), gold or platinum substrates [5]. At low current density conditions, nano-sized needles grow with the *b*-axis perpendicular to the substrate surface, following a homogeneous nucleation process, being controlled by diffusion. Using (001)-oriented silicon wafers, our group has reported the preparation of  $\text{Per}_2[\text{Au}(\text{mnt})_2]$  nanowires [6]. Nanowires were grown in the anodic compartment of an H-type electrochemical cell using perylene and  $[(n\text{-C}_4\text{H}_9)_4\text{N}][\text{Au}(\text{mnt})_2]$  as starting compounds. The oxidation of the perylene was performed at a constant current density of  $\sim 0.30 \mu\text{A}\cdot\text{cm}^{-2}$  at room temperature.  $\text{Per}_2[\text{Au}(\text{mnt})_2]$  nanowires exhibited a semiconducting behavior in the 100–298 K range and a room-temperature conductivity value of about  $0.020 \text{ S}\cdot\text{cm}^{-1}$ .

Amphiphilic molecules can control the growth of molecule-based conductors and allow the formation of nanoparticles [7]. In many cases, the molecule-based conductor contains at least one 5-membered heterocycle with two sulfur atoms. The amphiphilic 1-octanamine, *N*-(2-thienylmethylene) molecule (OATM, Figure 2) can afford two possibilities of interactions with the heterocycle, in favor of a better growth control of the nanoparticles:  $\pi$ - $\pi$  interactions if the heterocycle contains unsaturation and  $\text{S}\cdots\text{S}$  van der Waals interactions. Moreover, the long octyl chain can favor a better dispersion of the nanoparticles due to steric repulsions.

In this paper, we have explored the use of the amphiphilic OATM and the zwitterionic ionic liquid 4-(3-butyl-1-imidazolium)-1-butananesulfonate (BIBS, Figure 2) to control the growth of  $\text{Per}_2[\text{Au}(\text{mnt})_2]$  as nano-objects.

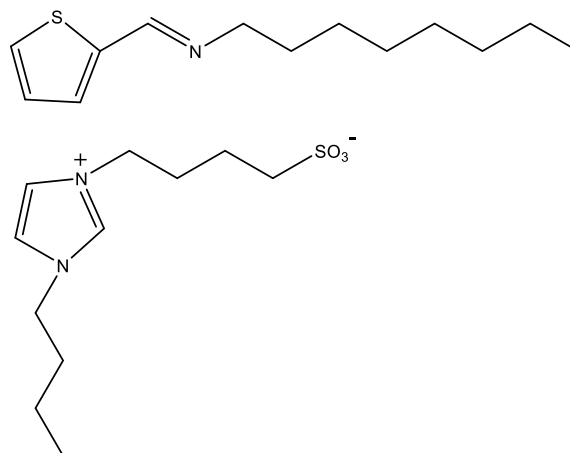


**Figure 2.** Formulas for OATM (above) and BIBS (below).

## 2. Experimental section

### 2.1. Materials

Solvents are degassed immediately before use. Perylene,  $[(\text{C}_2\text{H}_5)_4\text{N}]\text{Br}$ , sodium maleonitriledithiolate ( $\text{Na}_2\text{mnt}$ ), potassium tetrachloroaurate ( $\text{KAuCl}_4$ ), 2-thiophenecarboxaldehyde, octylamine, 1-butyl-3-methylimidazolium tetrafluoroborate  $[\text{BMIM}][\text{BF}_4]$ , 1-butyl-3-methylimidazolium hexafluorophosphate  $[\text{BMIM}][\text{PF}_6]$ , 1-butyl-3-methylimidazolium bis(trifluoromethylsulfonyl)imide  $[\text{BMIM}][(\text{CF}_3\text{SO}_2)_2\text{N}]$  and BIBS are commercially available and used without further purification.

### 2.2. Characterization

Elemental analyses are performed by the Microanalysis Service of LCC-CNRS. Nuclear magnetic resonance (NMR) of OATM is performed in dimethyl sulfoxide- $d_6$  at room temperature on a Bruker Avance 400 spectrometer. All chemical shifts for  $^1\text{H}$  are relative to tetramethylsilane. Infrared spectra are taken at room temperature (in KBr matrix) on a Perkin Elmer Spectrum GX spectrophotometer. Raman measurements are performed using a LabRAMHR800 (Jobin Yvon) set-up. The spectra are obtained at room temperature using the 632.8 nm line of a He-Ne laser. The incident beam is focused onto the sample through the  $\times 100$  optical microscope objective, giving a spot size of  $\sim 1 \mu\text{m}^2$ . The back-scattered light is collected through the same

objective, dispersed (single-grating spectrograph, 1800 grooves·mm<sup>-1</sup>, focal length  $f = 80$  cm) and then imaged onto a CCD detector (Andor DU420-OE). Using a laser power density of about  $1.7 \times 10^6$  W·cm<sup>-2</sup>, no degradation of the material is observed. For transmission electron microscopy (TEM), the samples are sonicated in ether and placed onto a holey carbon-copper grid. TEM experiments are performed on a JEOL Model JEM 1011 operating at 100 kV. Powder conductivity measurements are carried out on pressed pellets of pure powder materials (size: 3.14 mm<sup>2</sup> × 1 mm thick) without any grinding. The cylinders used to press the materials play the electrodes role. Resistance data acquisition is achieved using a Hewlett-Packard model 4263A LCR meter. Current–voltage ( $I$ – $V$ ) curves are acquired on an AFM Smarts SPM 1000 (AIST-NT) in conductivity mode using Au-coated cantilever tips (PPP-NCL Au-10 from Nanosensors, resonance frequency: 146–236 kHz, force constant: 21–98 N·m<sup>-1</sup>, tip radius: ~10 nm). The particles are dispersed on a gold substrate previously cleaned with acetone, water, and carefully dried.

### 2.3. Syntheses

[(C<sub>2</sub>H<sub>5</sub>)<sub>4</sub>N][Au(mnt)<sub>2</sub>] is prepared by addition of [(C<sub>2</sub>H<sub>5</sub>)<sub>4</sub>N]Br to a water solution of Na<sub>2</sub>mnt and KAUCl<sub>4</sub> at room temperature. Recrystallization is performed in a 1:2 (vol./vol.) mixture of acetone and isopropanol (yield: 35%; elemental analysis, calculated: C 31.7%; H 3.3%; N 11.6%, found C 31.7%; H 3.2%; N 11.4%). OATM is prepared as a pale yellow oil by the condensation reaction of 2-thiophenecarboxaldehyde and octylamine in toluene (yield: 91%; <sup>1</sup>H NMR (ppm): 0.84 (3H, t), 1.23–1.30 (10H, m), 1.56 (2H, tt), 3.48 (2H, t), 7.12 (1H, dd), 7.43 (1H, dd), 7.62 (1H, dd), 8.43 (1H, s)).

The synthesis of Per<sub>2</sub>[Au(mnt)<sub>2</sub>] nanoparticles is performed in a classical H-shaped electrocrystallization cell equipped with two platinum wire electrodes (length  $L = 1$  cm, diameter  $d = 1$  mm). The cathodic compartment is filled with [(C<sub>2</sub>H<sub>5</sub>)<sub>4</sub>N][Au(mnt)<sub>2</sub>] (20 mg, 0.03 mmol) solubilized in a mixture of 8 mL dichloromethane and 4 mL acetonitrile. The anodic compartment is filled with perylene (30 mg, 0.12 mmol), [(C<sub>2</sub>H<sub>5</sub>)<sub>4</sub>N][Au(mnt)<sub>2</sub>] (40 mg, 0.07 mmol) and OATM (70 µL, 0.30 mmol, *i.e.* 2.5 molar eq. *vs.* perylene) [or BIBS, 78 mg, 0.30 mmol]

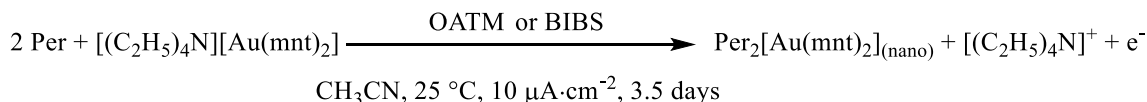
solubilized in a mixture of 8 mL dichloromethane and 4 mL acetonitrile. The electrolysis is conducted at room temperature under galvanostatic conditions (~10 µA·cm<sup>-2</sup>). The anodic solution is vigorously stirred during the entire electrolysis procedure (~3.5 days). The air-stable black powder of Per<sub>2</sub>[Au(mnt)<sub>2</sub>] is collected by filtration from the anodic compartment (Scheme 1). Yield: 40%. Elemental analysis, calculated: C 58.7 %; H 2.5 %; N 5.7 %, found C 58.4%; H 2.2%; N 5.8%. IR (cm<sup>-1</sup>): 3055 (ν<sub>CH</sub> ethylenic for perylene), 2222 and 2208 (ν<sub>CN</sub> for mnt<sup>2-</sup> ligands), 1536 and 1512 (ν<sub>C=C</sub>), 813 (ν<sub>C-S</sub>).

### 3. Results and discussion

The electrocrystallization technique under galvanostatic conditions and low current densities is the method of choice to grow single crystals of molecule-based conductors which are suitable for physical studies [8,9]. In the absence of stirring of the solution, the crystallographic quality of the product is much better. When the electrosynthesis is conducted in the presence of an amphiphilic molecule or an ionic species bearing bulky long carbon chains, the electrode can be rapidly passivated. A vigorous stirring is then necessary to favor the access of the electroactive species to the electrode.

We have performed the oxidation of perylene in the presence of [(C<sub>2</sub>H<sub>5</sub>)<sub>4</sub>N][Au(mnt)<sub>2</sub>], acting as both reactant and supporting electrolyte, at 10 µA·cm<sup>-2</sup> under stirring for 3.5 days. Transmission electron micrographs for the Per<sub>2</sub>[Au(mnt)<sub>2</sub>] shiny black powder collected from the anodic compartment evidence micro-sized crystals (Figure 3). We therefore note that the absence of a growth controlling agent in the solution is accompanied by the absence of size control of the crystallites at the nanometer scale.

When the oxidation of perylene is conducted in the presence of [(C<sub>2</sub>H<sub>5</sub>)<sub>4</sub>N][Au(mnt)<sub>2</sub>] and OATM (2.5 molar eq./perylene) at 10 µA·cm<sup>-2</sup> under vigorous stirring for 3.5 days, a black powder of Per<sub>2</sub>[Au(mnt)<sub>2</sub>] is isolated in the anodic compartment (see Section 2). Electron micrographs evidence nanocrystals exhibiting irregular shapes and sizes in the 35–100 nm range (Figure 4). Similar results are obtained for 5 molar eq. of OATM *vs.* perylene. The OATM molecule thus plays a crucial role in the control of the growth of Per<sub>2</sub>[Au(mnt)<sub>2</sub>] as nano-objects. We assume that a π stacking can occur between the



**Scheme 1.** Electrosynthesis of  $\text{Per}_2[\text{Au}(\text{mnt})_2]$  nanoparticles (anodic reaction).



**Figure 3.** Electron micrograph for  $\text{Per}_2[\text{Au}(\text{mnt})_2]$  in the absence of growth controlling agent (bar = 500 nm).

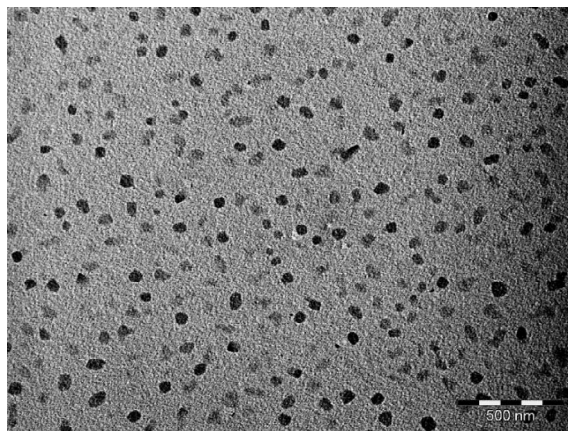


**Figure 4.** Electron micrograph for nanocrystals of  $\text{Per}_2[\text{Au}(\text{mnt})_2]$  grown in the presence of OATM (bar = 500 nm).

thiophene group of OATM and the  $\text{AuS}_2\text{C}_4$  ring of the  $\text{mnt}^{2-}$  ligand. Furthermore, OATM molecules can adsorb onto the platinum electrode surface. Therefore, the germination process of  $\text{Per}_2[\text{Au}(\text{mnt})_2]$  is more closely controlled at the electrode-solution interface, and the growth process is quickly blocked due to steric hindrance, leading to well dispersed nanocrystals. Finally, for higher current densities, namely,  $40 \mu\text{A}\cdot\text{cm}^{-2}$ , both well-dispersed nanocrystals and aggregates are observed. A faster growth rate thus implies a poorer control of the state of dispersion of the nanocrystals.

As said in the introduction, ionic liquids containing the 1-butyl-3-methylimidazolium cation,  $[\text{BMIM}]^+$ , are the most often used as growth controlling agents for the preparation of molecule-based conductors as nanoparticles. At low temperatures, the ionic liquid organized into nonpolar microdomains in which the confinement of the growing species is more efficient, affording small particles. The electrochemical oxidation of perylene in the presence of  $[(\text{C}_2\text{H}_5)_4\text{N}][\text{Au}(\text{mnt})_2]$  and  $[\text{BMIM}][\text{X}]$  where  $\text{X}^-$  stands for  $\text{BF}_4^-$ ,  $\text{PF}_6^-$  or  $(\text{CF}_3\text{SO}_2)_2\text{N}^-$  leads to  $\text{Per}_2\text{BF}_4$ ,  $\text{Per}_2\text{PF}_6$  or  $\text{Per}_2[(\text{CF}_3\text{SO}_2)_2\text{N}]$ .

The counter anion of  $\text{BMIM}^+$  prevails over the  $[\text{Au}(\text{mnt})_2]^-$  anion in the final product. To overcome this problem, we have therefore evaluated the use of the zwitterionic ionic liquid, *i.e.* BIBS (Figure 2), as both supporting electrolyte and growth controlling agent in the electrosynthesis of  $\text{Per}_2[\text{Au}(\text{mnt})_2]$ .

We have performed the oxidation of perylene in the presence of  $[(\text{C}_2\text{H}_5)_4\text{N}][\text{Au}(\text{mnt})_2]$  and BIBS (2.5 molar eq./perylene) at  $10 \mu\text{A}\cdot\text{cm}^{-2}$  under stirring for 3.5 days. A black powder of  $\text{Per}_2[\text{Au}(\text{mnt})_2]$  is isolated in the anodic compartment (see Section 2). Electron micrographs evidence well dispersed roughly spherical nanoparticles with sizes ranging from 10 to 40 nm (Figure 5). In comparison with OATM, the BIBS allows a better control of the morphology of the particles (spherical *vs.* irregular shapes). Furthermore, smaller particles are grown (10–40 nm *vs.* 35–100 nm).  $\text{Per}_2[\text{Au}(\text{mnt})_2]$  nanoparticles obtained in the presence of BIBS are very similar to those previously described for another bis(dithiolene) complex, *i.e.*,  $\text{TTF}[\text{Ni}(\text{dmit})_2]_2$  grown with  $[\text{BMIM}][\text{X}]$ , as growth controlling agent [2]. The BIBS could play a double role in the controlled growth of  $\text{Per}_2[\text{Au}(\text{mnt})_2]$  as nanoparticles. As for

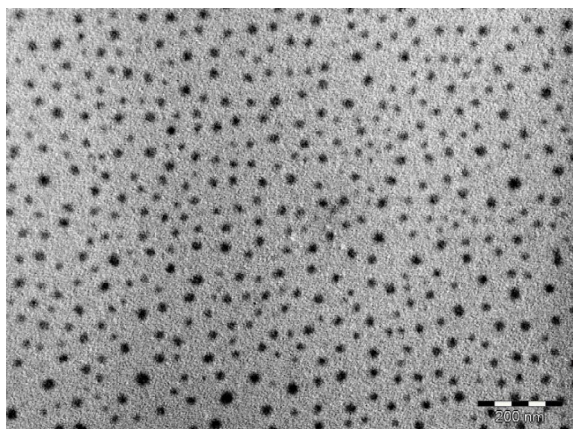


**Figure 5.** Electron micrograph for nanoparticles of  $\text{Per}_2[\text{Au}(\text{mnt})_2]$  grown in the presence of BIBS (bar = 200 nm).

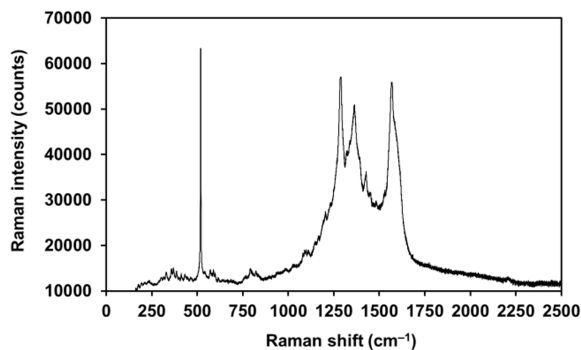


**Figure 6.** Raman spectrum for  $\text{Per}_2[\text{Au}(\text{mnt})_2]$  nanoparticles.

OATM,  $\pi$ - $\pi$  interactions between the imidazolium cycle of the BIBS and the  $\text{AuS}_2\text{C}_4$  ring of the  $\text{mnt}^{2-}$  ligand can occur. Furthermore, at the electrode surface, the BIBS could stabilize the  $\text{Per}^+$  ion *via* electrostatic attraction with the sulfonate  $\text{SO}_3^-$  group.

The Raman spectrum for  $\text{Per}_2[\text{Au}(\text{mnt})_2]$  nanoparticles (Figure 6) is dominated by the C=C stretching modes for both the perylene molecules and the dithiolate ligands (in the 1320–1600  $\text{cm}^{-1}$  range). Low frequency bands at 370, 518, and 800  $\text{cm}^{-1}$  are assigned to Au-S stretching mode,  $\text{AuS}_2\text{C}_2$  ring deformation mode, C-S stretching mode, respectively [10].

$\text{Per}_2[\text{Au}(\text{mnt})_2]$  single crystals present an electrical conductivity of 700  $\text{S}\cdot\text{cm}^{-1}$  along the stacking axis (*b*) at 25 °C [11]. For  $\text{Per}_2[\text{Au}(\text{mnt})_2]$  nanoparticles

described in this paper, the conductivity at room temperature is found to be of about 0.025  $\text{S}\cdot\text{cm}^{-1}$ . This value is in agreement with those reported for  $\text{TTF}[\text{Ni}(\text{dmit})_2]_2$  nanopowders prepared in the presence of BMIM-based ionic liquids (in the 0.01–1  $\text{S}\cdot\text{cm}^{-1}$  range) [1]. The conductivity of a compressed pellet of a nanoparticle powder is the result of two main contributions: the conductivity of the particles (exhibiting random crystallographic orientations) themselves and the conductivity of the boundaries between them. The absence of a preferential crystallographic orientation of the particles within the nanopowder and the resistive boundaries between the particles explain a much lower conductivity value than that for single crystals. Figure 7 shows the *I*-*V* curve of an individual 40 nm high nanoparticle using conductive atomic force microscopy (sample prepared in the presence of BIBS). The deviation from the linear ohmic behaviour that would be expected for a metallic nanoparticle arises from the involved boundaries, such as tip-nanoparticle and substrate-nanoparticle. The observed energy gap is about 0.26 eV. A least-squares fit of the region corresponding to positive bias voltages (from 0.00 to 0.50 V) is shown on Figure 7. The fit is obtained using the Shockley diode equation:

$$I = I_0 \left[ e^{\frac{V}{V_0}} - 1 \right]$$

where  $I_0$  represents the saturation current and  $V_0$  the threshold voltage (energy barrier). From the fit, we obtain  $I_0 = 19.3 \pm 1.1$  pA and  $V_0 = 0.149 \pm 0.03$  V (coefficient of determination:  $R^2 = 0.993$ ). The activation energy barrier extracted from the fit (about 0.15 eV) is relatively consistent with half of the energy gap ( $0.26/2 = 0.13$  eV). For the sample prepared in the presence of OATM, *I*-*V* curves are noisy and asymmetric in shape, the positive bias voltages being 2–3 times higher than the negative ones (in absolute value).

#### 4. Conclusion

In this paper, we have described the first nanoparticles of the metal-organic conductor  $\text{Per}_2[\text{Au}(\text{mnt})_2]$ . The growth controlling agents evaluated in this study, namely, OATM and BIBS, prevented the preparation of  $\text{Per}_2[\text{Au}(\text{mnt})_2]$  as micro-sized crystals. Irregularly shaped nanocrystals are grown in the presence



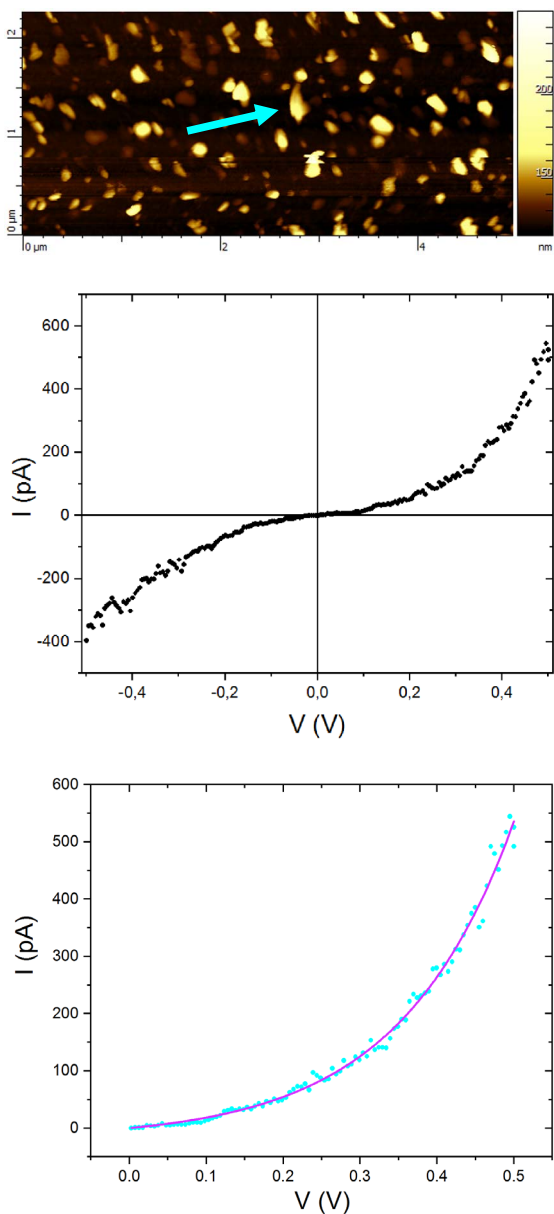


**Figure 7.** Topographic image for  $\text{Per}_2[\text{Au}(\text{mnt})_2]$  nanoparticles prepared with BIBS (top),  $I$ - $V$  curve for the particle indicated by the arrow (middle), least-squares fit of the region corresponding to positive bias voltages (down).

of OATM, whereas spherical nanoparticles are obtained if the zwitterionic ionic liquid BIBS is used. It has been reported that  $\text{Per}_2[\text{Au}(\text{mnt})_2]$  exhibits a

fairly good thermopower value of  $S = 40 \mu\text{V}\cdot\text{K}^{-1}$  [12]. Moreover, the thermal conductivity  $\lambda$  is very low for organic-based conductors as nanoparticles [13]. As the thermoelectric efficiency of a material is evaluated by its figure of merit  $ZT$  in which  $S^2$  is in the numerator and  $\lambda$  in the denominator,  $\text{Per}_2[\text{Au}(\text{mnt})_2]$  nanoparticles described in this paper could be interesting as one of the components for organic-based thermoelectric devices. Furthermore, our study opens the way to the potential preparation of nanoparticles of  $\text{Per}_2[\text{M}(\text{mnt})_2]$  systems in which  $\text{M}^{\text{III}}$  is a magnetic center such as  $\text{Ni}^{\text{III}}$ ,  $\text{Pd}^{\text{III}}$  or  $\text{Pt}^{\text{III}}$ . Such systems as nanoparticles could be interesting for fundamental physical studies.

## References

- [1] D. de Caro, K. Jacob, C. Faulmann, J.-P. Legros, F. Senocq, J. Fraxedas, L. Valade, *Synth. Met.*, 2010, **160**, 1223-1227.
- [2] D. de Caro, C. Faulmann, L. Valade, K. Jacob, I. Chtioui, S. Foulal, P. de Caro, M. Bergez-Lacoste, J. Fraxedas, B. Ballesteros, J. S. Brooks, E. Steven, L. E. Winter, *Eur. J. Inorg. Chem.*, 2014, **8**, 4010-4016.
- [3] J. S. Brooks, D. Graf, E. S. Choi, M. Almeida, J. C. Dias, R. T. Henriques, M. Matos, *Curr. Appl. Phys.*, 2006, **6**, 913-918.
- [4] D. Graf, J. S. Brooks, M. Almeida, J. C. Dias, S. Uji, T. Terashima, M. Kimata, *Europhys. Lett.*, 2009, **85**, 27009-27013.
- [5] M. L. Afonso, R. A. L. Silva, M. Matos, A. S. Viana, M. F. Montemor, M. Almeida, *Langmuir*, 2012, **28**, 4883-4888.
- [6] J.-P. Savy, D. de Caro, C. Faulmann, L. Valade, M. Almeida, T. Koike, H. Fujiwara, T. Sugimoto, J. Fraxedas, T. Ondarçuhu, C. Pasquier, *New J. Chem.*, 2007, **31**, 519-527.
- [7] D. de Caro, C. Faulmann, L. Valade, "Nanoparticles of Organic Conductors", in *Molecular Materials: Preparation, Characterization, and Applications* (S. Malhotra, B. L. V. Prasad, J. Fraxedas (dir. publ.), eds.), CRC Press, Boca Raton, 2017, 127-149.
- [8] P. Cassoux, L. Valade, P.-L. Fabre, "Fundamentals: Ligands, Complexes, Synthesis, Purification and Structure", in *Comprehensive Coordination Chemistry II: From Biology to Nanotechnology* (A. B. P. Lever (dir. publ.), ed.), Elsevier, Amsterdam, 2003, 761.
- [9] P. Batail, K. Boubekeur, M. Fourmigué, J.-C. P. Gabriel, *Chem. Mater.*, 1998, **10**, 3005-3015.
- [10] M. K. Johnson, "Vibrational Spectra of Dithiolene Complexes", in *Dithiolene Chemistry Synthesis, Properties, and Applications* (E. I. Stiefel (dir. publ.), ed.), John Wiley & Sons, Hoboken, 2004, 213-266.
- [11] M. Almeida, R. T. Henriques, "Perylene Based Conductors", in *Handbook of Organic Conductive Molecules and Polymers* (H. Singh Nalwa (dir. publ.), ed.), vol. 1, John Wiley & Sons, Chichester, 1997, 87.
- [12] M. Matos, G. Bonfait, I. C. Santos, M. L. Afonso, R. T. Henriques, M. Almeida, *Magnetochemistry*, 2017, **3**, 22-34.
- [13] I. Chtioui-Gay, C. Faulmann, D. de Caro, K. Jacob, L. Valade, P. de Caro, J. Fraxedas, B. Ballesteros, E. Steven, E. S. Choi,



M. Lee, S. M. Benjamin, E. Yvenou, J.-P. Simonato, A. Carella,  
*J. Mater. Chem. C*, 2016, **4**, 7449-7454.